Arabian Journal of Chemistry (2023) **16**, 104710

King Saud University

Arabian Journal of Chemistry

www.ksu.edu.sa
www.sciencedirect.com

ORIGINAL ARTICLE

Synthesis of *Rumex hastatus*-based silver nanoparticles induced the inhibition of human pathogenic bacterial strains

Saddaf Rashid [a], Rafiq Ahmad [a,*], Muhammad Azeem [b], Dunia A. Al Farraj [c], Sabaz Ali Khan [a], Mohamed Soliman Elshikh [c], Arshad Mehmood Abbasi [d,e,*]

[a] *Department of Biotechnology, COMSATS University Islamabad, Abbottabad Campus, 22060 Abbottabad, Pakistan*
[b] *Department of Chemistry, COMSATS University Islamabad, Abbottabad Campus, 22060 Abbottabad, Pakistan*
[c] *Department of Botany and Microbiology, College of Science, King Saud University, Riyadh 11451, Saudi Arabia*
[d] *Department of Environmental Sciences, COMSATS University Islamabad, Abbottabad Campus, 22060 Abbottabad, Pakistan*
[e] *University of Gastronomic Sciences of Pollenzo, Piazza V. Emanuele II, I-12042, Bra/Pollenzo, Italy*

Received 19 October 2022; accepted 20 February 2023
Available online 25 February 2023

KEYWORDS

Rumex hastatus;
AgNPs synthesis;
Antibacterial activity;
Pathogenic bacterial strains;
FTIR;
SEM

Abstract The development of antibiotic resistance in pathogenic bacterial strains has drawn attention to the quest for new natural antibacterial drugs. Therefore, in the present study, extracts of *Rumex hastatus* leaves were obtained in methanol and water, and *R. hastatus*-based silver nanoparticles (AgNPs) were synthesized. Structural and functional properties of synthesized silver nanoparticles were determined by UV–vis spectroscopy, XRD, FTIR and SEM. The synthesized AgNPs and crude extracts were tested to check their antibacterial potential against human pathogenic bacterial strains of *Staphylococcus aureus*, *Staphylococcus haemoliticus, Bacillus cereus, Escherichia coli*, *Salmonella typhi and Pseudomonas aeruginosa* in well diffusion and broth dilution methods. The present investigation has revealed for the first time that the broth dilution method was found more reproducible than that of the well diffusion method even at lower concentrations of AgNPs and crude extracts. UV– Vis spectroscopic analysis of AgNPs revealed a peak at 367 nm. XRD pattern showed a face-centered cubical to the spherical structure of AgNP crystals. FTIR analysis revealed that flavonoids and terpenoids are responsible for the reduction of $AgNO_3$ to Ag^+. SEM analysis determined the spherical structure and 51 nm average diameter of nanoparticles. The antibacterial

* Corresponding authors.
E-mail addresses: sadafrashid63@yahoo.com (S. Rashid), drrafiq@cuiatd.edu.pk (R. Ahmad), muhazeem@cuiatd.edu.pk (M. Azeem), dfarraj@ksu.edu.sa (D.A. Al Farraj), sabaz@cuiatd.edu.pk (S.A. Khan), melshikh@ksu.edu.sa (M.S. Elshikh), amabbasi@cuiatd.edu.pk (A.M. Abbasi).

Peer review under responsibility of King Saud University.

Production and hosting by Elsevier

https://doi.org/10.1016/j.arabjc.2023.104710

activity of *R. hastatus*-based (AgNPs) was found to be significantly higher than aqueous plant extract and silver nitrate alone. Bacterial growth was inhibited by *R. hastatus*-based AgNPs in a dose-dependent manner. To our knowledge, silver nanoparticles (AgNPs) of *R. hastatus* were synthesized and characterized for the first time in this study and, based on the findings of current research work *R. hastatus* extract-based silver nanoparticles are suggested to be used as an antibacterial drug instead of synthetic drugs for the treatment of various human diseases/infections caused by the tested bacterial strains.

1. Introduction

Treatment with medicinal plants is as old as mankind and is utilized by different communities since ancient times to prevent a variety of diseases (Petrovska 2012, Ogbuewu et al., 2011, Lulekal et al., 2013). World Health Organization (WHO) declared that about 65–80 % of the world's population in developing nations predominantly depends on plants for their primary health care due to their socio-economic issues as they could not afford modern medical facilities (Calixto 2005, Kayani et al., 2014, Ahmed et al., 2015, Roope et al., 2019, Dildora Ergashevna and Honbuvi Khakimovna 2022).

Rumex hastatus is a herbaceous plant; it is distributed in Pakistan, China and Afghanistan. It can be used as a flavoring agent as leaves of *R. hastatus* have a pleasant acidic taste and are hence used in chutneys and pickles. *R. hastatus* is used as a medicine too because of its therapeutic abilities. It is used as a laxative and tonic to cure rheumatism, piles, skin diseases, and blood pressure while as herbal medicine to prevent sexually transmitted diseases like AIDS (Sahreen et al., 2011). High phenolic and flavonoid content of methanolic extracts of *R. hastatus* leaves is directly associated with high DPPH scavenging activity *i.e.,* it has increased antioxidant potential (Sulaiman and Balachandran 2012). Leaves and shoots are refrigerant and diuretic (Hameed and Dastagir 2009) while roots against dysentery, diuretic, wounds, neoplasm, jaundice *etc* (Shakuntala et al., 2011). Juice of *R. hastatus* can be used to treat tonsillitis, sore throat and blood pressure (Ahmed et al., 2015). Various studies on *R. hastatus* have also shown anti-angiogenic activity, anti-tumor activity and anti-cholinesterase properties (Ahmed et al., 2016).

Silver nanoparticles have broad spectrum use in the field of biomedical sciences for their antimicrobial activity (Valli and Vaseeharan 2012, Li et al., 2013, De Ghosh et al., 2014, Ibrahim 2015, Khan et al., 2022, Gökşen Tosun et al., 2022), healing of burned patients (Singh et al., 2014, Jadhav et al., 2016, Martínez-Higuera et al., 2021), anticancerous activity (Kaplan et al., 2022, Ijaz et al., 2022), wastewater treatment ((Mehwish, 2021 #135)Khan, 2022 #134), DNA sequencing (Zhang et al., 2023) and targeted drug delivery (Prasad et al., 2011, Prasad and Swamy 2013, Jain et al., 2021, Gulia et al., 2022). In the modern age surgical instruments, food covering sheets and canes of food items are coated with nanoparticles to avoid them from pathogens (Sharma et al., 2009, Prasad et al., 2011, Prasad et al., 2012, Shimpi et al., 2022, Rezić 2022). Nanomaterials are useful in many techniques such as molecular imaging, fluorescence imaging and multimodal imaging (Habeeb Rahuman et al., 2022). Silver nanoparticles are extensively used in biological studies as they are cost-effective compared to physical and chemical processes, eco-friendly, more efficient against microbes, and safe to use (Savithramma et al., 2011, Alharbi et al., 2022, Chakravarty et al., 2022). Products involving the use of silver nanoparticles are US FDA, US EPA, Korea's Testing, SIAA of Japan and Research Institute for Chemical Industry and FITI Testing and Research Institute approved, which are some major accredited bodies. The plant products exhibit remarkable reducing potential to synthesize silver nanoparticles, the only nontoxic and ecofriendly way of nanoparticle synthesis in the field of nanotechnology (Ijaz et al., 2022, Kaplan et al., 2021).

Selected gram-positive and gram-negative bacteria including *Staphylococcus aureus*, *Staphylococcus haemoliticus, Bacillus cereus, Escherichia coli*, *Salmonella typhi and Pseudomonas aeruginosa* are the causative agents of different infectious diseases like urinary tract infection, typhoid fever, food poisoning, diarrhea, gastrointestinal infections, rheumatic heart diseases, oral infections and respiratory infections (Gellatly and Hancock 2013, Marzano et al., 2003, Croxen et al., 2013, Kotiranta et al., 2000, Gunn and Davis 1988).

Published literature has revealed that *R. hastatus* has not been studied for its antimicrobial activities using green silver nanoparticles. Therefore, the present study is focused on the synthesis of green silver nanoparticles using an aqueous extract of total *R. hastatus* as well as different parts of *R. hastatus* to estimate their antimicrobial potential.

2. Materials and methods

2.1. Collection and identification of plant material

R. hastatus was collected in April 2018 from 34.1688° N, 73.2215° E, Abbottabad. Plant material was identified by Dr. Arshad Mahmood Abbasi, Department of Environmental Sciences, COMSATS University Islamabad, Abbottabad Campus. A voucher specimen (CUHA-92) of *R. hastatus* was also deposited at the Herbarium of Pakistan Museum of Natural History Islamabad. Collected leaves of the *R. hastatus* were washed with tap water to remove the dust and other superficial contamination and subsequently dried in shade for 15 days. Dried leaves were ground into fine powder to prepare aqueous extracts using two types of maceration, which are described below.

2.2. Extract preparation

*A s*imple maceration process (Bennour et al., 2020) was carried out to obtain methanolic leaf extracts of *R. hastatus*. In this process, 50 g of ground leaves were soacked in 300 mL methanol. The mixture was kept on shaking at 1000 rpm for 3 days. The sample was filtered with whatmann No. 1 filter paper, then concentrated at reduced pressure at 30–40 °C using a rotary evaporator to determine antibacterial activity.

2.3. Biochemical analysis

2.3.1. Determination of total phenolic and flavonoid content

The total phenolic content of *R. hastatus* leaves was determined by the Folin-Ciocalteu method (Martins et al., 2021). The absorbance was recorded at 765 nm by using a double beam BMS (UV-1602) spectrophotometer. The average result of total phenolic content was presented as gallic acid equivalent (GAE) mg/g of dry weight. Total flavonoid content

was determined by $AlCl_3$ (Aluminum chloride) colorimetric method (Chen and Zhou 2022). The absorbance was measured at 510 nm and results were calculated as quercetin equivalent QE mg /g of dry weight.

2.3.2. Free radical scavenging activity of plant crude extract

Free radical scavenging activity of *R. hastatus* leaves extract was measured using 1, 1- diphenyl-2-picryl hydrazyl (DPPH) according to the modified method described by (Adebayo et al., 2010). UV–vis spectrophotometer was used to measure the absorbance of the solution at 517 nm. Percent DPPH inhibition was calculated by following formula:

$$\%DPPHInhibition = \frac{A_{Blank} - A_{Sample}}{A_{Blank}} \times 100$$

Where A indicates Absorbance.

2.4. Antibacterial activity

2.4.1. Sample preparation

300 mg of *R. hastatus* crude extract was dissolved in 1 mL of dimethyl sulphoxide (DMSO). This stock solution was used to assess the antibacterial potential of *R. hastatus* against disease-causing pathogens. Streptomycin was diluted as 1 mg/ml in double distilled water for a comparative study.

2.4.2. Test Organisms: Bacterial strains and inoculum preparation

Six bacterial strains were used to test the efficiency of *R. hastatus* extracts. *Staphylococcus aureus* (KX262679), *Staphylococcus haemoliticus* (KX262673) and *Bacillus cereus* (KX262674) as gram-positive bacteria and *Escherichia coli* (ATCC 10536), *Salmonella typhi* (ATCC 6539) *and Pseudomonas aeruginosa* (ATCC 9027) that belong to the category of gram-negative bacteria. Microbial strains were collected from the Institute of Environmental Science and Engineering, National University of Science and Technology, Islamabad and Ayub Medical Complex, Abbottabad. These strains were grown in nutrient broth and then cultured on nutrient agar to maintain them at a 37 °C incubator overnight. The next day each bacterial colony was mixed in 3 mL distilled water, vortexed and optical density was made equal to 0.5 using a spectrophotometer on 600 nm wavelength.

2.4.3. Agar well diffusion method

The antibiotic activity of *R. hastatus* was assessed using the agar well diffusion method (Sen and Batra 2012, Chauhan et al., 2017). Agar plates were made by using autoclaved nutrient media (as per the manufacturer's instructions). DMSO was used as negative-control and streptomycin (1 mg/ml) was used as positive-control. The zone of inhibition was measured in millimeters for antibacterial activity.

2.4.4. Broth dilution method

Antibacterial activity of *R. hastatus* was also tested using modified broth dilution method (Wiegand et al., 2007). Briefly, bacterial colonies were suspended in 0.9 % saline solution and optical density was set to 0.5 at 600 nm using nanodrop (Colibri Spectrophotometer) to get 10^7–10^8 colony forming units (CFU). Bacterial suspensions were further diluted to get 10^3 – 10^4 CFU/ml, and 495 µl of this suspension was poured in Eppendorf tubes. An aliquot of 5 µl extract of *R. hastatus* or DMSO or streptomycin was added to them. Eppendorf tubes containing mixture of bacterial suspension and test extract/-controls were vortexed and incubated at shaking incubator for 30 min at 37 °C. After incubation, 100 µl of mixture was further spread on agar plates (two replicates) and again incubated at 37 °C for 10 h. Number of live bacteria was determined by counting the number of bacterial colonies on each plate, equal to colony forming unit (CFU). Growth inhibition was presented as % inhibition by using following formula:

$$\%\,\text{Inhibition} = \frac{\text{CFU in control} - \text{CFU in test}}{\text{CFU in control}} \times 100$$

2.5. Synthesis of silver nanoparticles

Plant based synthesis of silver nanoparticles (AgNPs) was carried out according to the method described by (Chung et al., 2016). Shortly, 4 % aqueous extract of *R. hastatus* leaves was prepared and kept in a water bath at 50–55 °C for 15–20 min. Crude extract was filtered with Whatmann No. 1 filter paper and stored in refrigerator at 4 °C. Afterwards, 1 mL of crude leaf extract was added to 9 mL sterile distilled water and the 10 mL from this extract was added to 90 mL of 0.1 mM $AgNO_3$ solution and incubated at 37 °C for 24 h. AgNPs were reduced to silver ions; changing their color from light yellow to dark brown that showed the synthesis of green silver nanoparticles. Sample was then transferred to a round bottom flask for continuous stirring and heating at 100 °C for 15 min. After heating, the solution was centrifuged for 15 min at 6000 rpm and the resulting nanoparticles mixture was collected after discarding the supernatant. These nanoparticles were dried at room temperature for 2–3 days.

2.5.1. Characterization of AgNPs

Bio reduction of silver ions and synthesis of AgNPs was monitored by using BMS (UV-1602) UV–Visible spectrophotometer (Rashid et al., 2019). Crystalline structure of synthesized AgNPs was determined and confirmed using X-ray diffraction (BRUKER D8 X-ray diffractometer). Average crystallite size of synthesized AgNPs was calculated using Scherrer's formula (Patterson, 1993). Morphological and chemical analyses of synthesized AgNPs were carried out using FTIR and JEOL 7001F FEG-SEM (REEQ/711/CTM/2005) equipped with EDX detector.

2.5.2. Antibacterial activity of AgNPs

Antibacterial potential of synthesized AgNPs was assessed by agar well diffusion method (as described earlier). Wells were loaded with five different concentrations of synthesized AgNPs *i.e.,* 1, 2, 3, 4 and 5 mg/ml. $AgNO_3$ (1 mM), plant extract were used to assess individual antibiotic activity, standard antibiotic (streptomycin 1 mg/ml) as a positive control and H_2O was used as negative control. After 24 h incubation, zone of inhibition was recorded.

2.6. Statistical analysis

The data were demonstrated as mean and standard deviation of three separate experiments with five replicates. One way

ANOVA with Tukey's HSD *post hoc* test was used to find the significant difference between control and test sample and the difference between bacterial growth inhibition when treated with different concentration of synthesized AgNPs. This statistical analysis was carried out using SPSS IBM statistics 23 software.

3. Results

3.1. Phenolic and flavonoid content of *Rumex hastatus*

Crude extract of the leaves showed higher concentration (105.05 ± 2.13) mg of GAE/g of total phenolic content. Total flavonoid content of crude extract (Table 1) was determined from the calibration curve (R^2 = 0.9902), was (110 ± 29) mg QE/g.

3.2. DPPH scavenging activity of Rumex hastatus extract

Crude extract exhibited 88 % DPPH scavenging activity at a concentration of 2000 µg plant extract as presented in Table 1.

3.3 Growth Inhibition of Pathogenic Strains by Well Diffusion. In well diffusion method all bacterial strains were susceptible towards crude extracts of *R. hastatus* leaves except *S. haemolyticus* (Table 2). Leaves of *R. hastatus showed* zone of inhibition ranged from 10 to 15 mm against *E. coli*, *S. aureus, P. aeruginosa, B. cereus* and *S. typhi*. Significant difference ($P < 0.05$) was observed between growth inhibition of pathogenic strains with crude leaf extract of *R. hastatus* and synthetic drug, streptomycin (Positive control), completely inhibited the growth of all tested strains at a concentration 1 mg/ml as shown in Table 2.

3.3. % Inhibition of pathogenic strains by broth dilution method

While testing through broth dilution method, all tested strains were found to be sensitive towards crude extracts of *R. hastatus* leaves. However, the CFU inhibition activity was highest against *P. aeruginosa, S. typhi, B. cereus* and *E. coli* ranging from 82 to 99 % that was significantly higher ($P < 0.05$) than streptomycin. *S. aureus* and *S. haemolyticus* were significantly ($P < 0.05$) less susceptible 44–74 % towards crude extract of *R. hastatus* leaves compared with positive control (Table 3). Growth of *P. aurigonosa* was completely inhibited (99 ± 1) % and *S. haemolyticus* was least inhibited (44 ± 12) % by crude extract of *R. hastatus* leaves.

3.4. UV – Visible Spectrum of AgNPs with respect to Time

Aqueous plant extract when mixed with $AgNO_3$, silver ion started to reduce by the plant extract which was observed by the change in color of the reaction mixture. The color of the extract changed from milky to light brown during the first hour and turned to dark brown after 5 h of incubation after which no color change was observed. UV–Visible spectra of the reaction mixture after regular time intervals are shown in Fig. 1, that showed a specific peak at 367 nm.

Table 1 Total phenolic and flavonoid content of methanolic extract of R. hastatus leaves.

Parameters	Methanol extract
Total phenolic[b]	105.05 ± 2.13
Total flavonoid[a]	110.2 ± 29.2
DPPH scavenging activity[c]	88.05 ± 0.15

[a] mg of GAE / g of TPC; [b] mg of QE / g of TFC; [c] % Inhibition.

Table 2 Antibiotic activity of crude extract of *R. hastatus* leaves using well diffusion method.

Strains	Zone of inhibition (Average ± S.D) mm		
	R. hastatus (Crude extract)	Streptomycin (Positive control)	DMSO (Negative control)
Pseudomonas aeruginosa	12.1 ± 1^{Ab}	23.9 ± 1^{Aa}	0 ± 0^{c}
Salmonella typhi	11.8 ± 1^{Ab}	20.8 ± 1^{Ba}	0 ± 0^{c}
Escherichia coli	12.0 ± 2^{Ab}	19.4 ± 1^{Ca}	0 ± 0^{c}
Staphylococcus aureus	12.2 ± 2^{Ab}	22.6 ± 1^{Aa}	0 ± 0^{c}
Staphylococcus haemolyticus	0 ± 0^{Bb}	23.1 ± 1^{Aa}	0 ± 0^{b}
Bacillus cereus	11.2 ± 1^{Ab}	22.7 ± 1^{Aa}	0 ± 0^{c}

Different small letters in superscript revealed the significant difference ($P < 0.05$) among the zone of inhibition of bacteria with crude leaf extract of *R. hastatus*, positive and negative controls. Different capital letters represent the significant difference ($P < 0.05$) among all tested strains.

Table 3 Antibiotic activity of crude extract of *R. hastatus* leaves using broth dilution method.

Strains	% Inhibition (Average ± S.D)		
	R. hastatus (Crude extract)	Streptomycin (Positive control)	DMSO (Negative control)
Pseudomonas aeruginosa	99 ± 1^{Aa}	80 ± 3^{Bb}	0 ± 0^{c}
Salmonella typhi	98 ± 0^{Aa}	19 ± 4^{Cb}	0 ± 0^{c}
Escherichia coli	86 ± 0^{Aa}	72 ± 4^{Bb}	0 ± 0^{c}
Staphylococcus aureus	74 ± 4^{Bb}	95 ± 1^{Aa}	0 ± 0^{c}
Staphylococcus haemolyticus	44 ± 12^{Bb}	44 ± 4^{Ca}	0 ± 0^{c}
Bacillus cereus	82 ± 1^{Ab}	97 ± 5^{Aa}	0 ± 0^{c}

Different letters in superscript revealed the significant difference ($P < 0.05$) among % inhibition of bacteria with crude leaf extract of *R. hastatus*, positive and negative controls. Different capital letters represent the significant difference ($P < 0.05$) among all tested strains within a treatment.

3.5. XRD analysis of AgNPs

X-ray differation pattern of AgNPs synthesized by the reduction of Ag ions with aqueous leaf extract of *R. hastatus* revealed five characteristic peaks in whole spectrum of 2θ val-

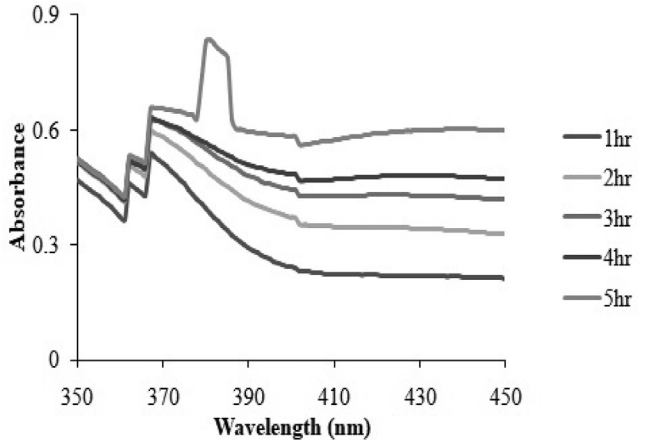

Fig. 1 UV– Visible spectrum of synthesized silver nanoparticles at different time intervals.

ues ranging from 10 to 80. According to Scherrer's formula average crystallite size of synthesized AgNPs is 85 nm ranging from 36 to 100 nm. In XRD pattern five Bragg's reflections at 29.70°, 32.83°,39.14°, 53.84° and 62.04° (Fig. 2) were recorded, corresponding to 11, 200, 311 and 220 for silver respectively.

3.6. FTIR analysis of synthesized AgNPs

FTIR spectrum of synthesized AgNPs was carried out to identify the presence of possible functional groups within the biomolecules that bind to the surface of silver for its bioreduction. The prominent peaks at infrared spectrum detected in *R. hastatus* based AgNPs were compared with standard values to identify functional groups. FTIR spectrum showed stretching frequencies at five different regions *i.e.* 3215, 2364, 1580, 1290 and 800 cm^{-1} as shown in Fig. 3.

3.7. SEM & EDS analysis of AgNPs

SEM analysis of *R. hastatus* based AgNPs revealed that all nanoparticles were spherical in shape. The average size of

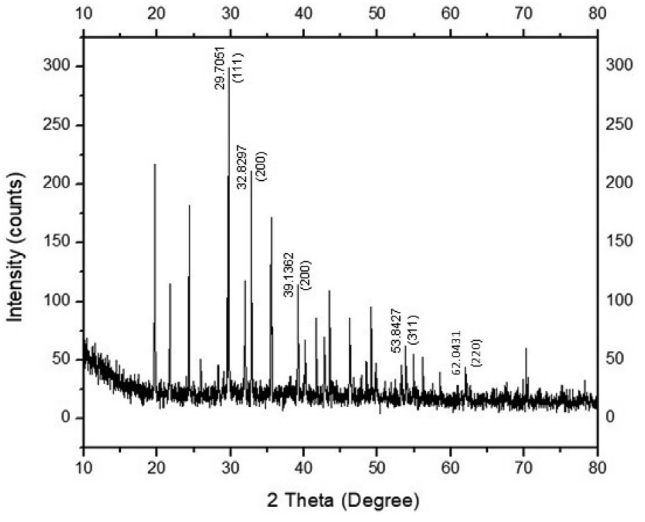

Fig. 2 XRD pattern of AgNPs indicating the facets of crystalline silver after bio-reduction.

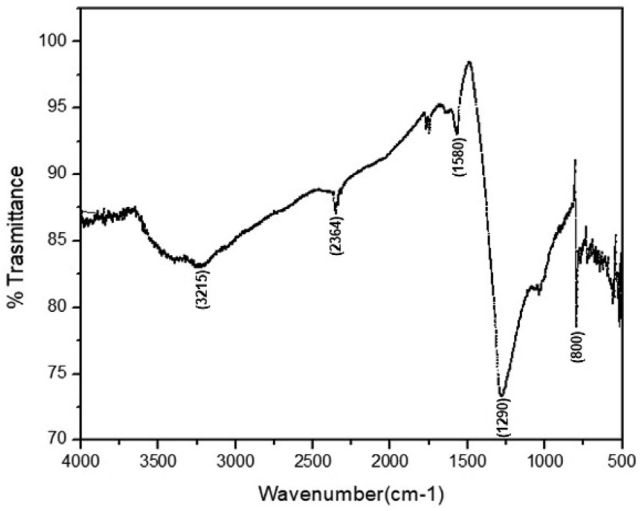

Fig. 3 FTIR spectrum of freeze dried sample of *R. hastatus* based AgNPs.

synthesized AgNPs was 51 nm in 500 nm area of SEM image, evident in Fig. 4A. Energy dispersive X-ray spectroscopy (EDS) analysis was carried out to confirm the presence of silver metal in the synthesized nanoparticles. Sharp peak at 3 KeV demonstrated the existence of elemental silver in the nanoparticles as shown in Fig. 4B.

3.8. Antibacterial activity of Rumex hastatus based AgNPs

Aquous extract of *R. hastatus* was found to have no antibacterial potential against all tested strains. Increasing trend of zone of inhibition in all tested strains was detected as the concentration of AgNPs increased, as revealed in the Fig. 5A-F. *P. aurigonosa* was found to be more suceptible at all AgNPs concentrations,with zone of inhibition ranging from 19.4 to 25.3 mm, when compared with other pathogenic strains as shown in Fig. 5A. Significantly ($P < 0.05$)greater zone of inhibition was observed at 5 mg/ml in comparison with controls ($AgNO_3$ and streptomycin) and lower concentrations of AgNPs. Inhibition zone of AgNPs was observed to be slightly more than that of $AgNO_3$ and aqueous leaf extract of *R. hastatus*.*S. typhi, E. coli, S. aureus, S. haemolyticus* and *B. cereus* have shown slightly increasing zone of inhibition as the concentration of AgNPs increases (Fig. 5B-F). Except *E. coli*and *B. cereus*,all other bacteria were significantly ($P < 0.05$) inhibited by AgNPs as compared to $AgNO_3$ (Fig. 5C & F).

4. Discussion

Pathogenic bacteria are causing lot of diseases in human beings particularly in developing countries and Plants and their extracts have been used to inhibit these pathogens from centuries (Yadav et al., 2017). The pathogenic bacteria used in this study are causing different diseases in humans (Gellatly and Hancock 2013, Marzano et al., 2003, Croxen et al., 2013, Ashebir and Ashenafi 2007). Current research work has revealed that crude extract of *R. hastatus* leaves was rich in total phenolic content which was supported by (Sahreen et al., 2011). Reported literature about

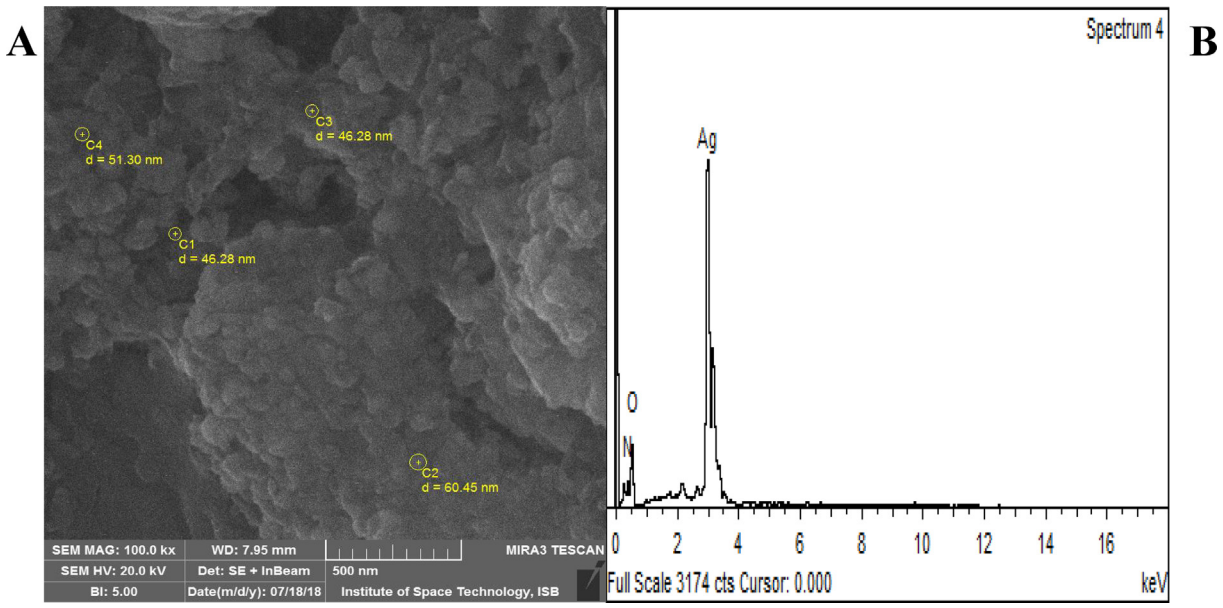

Fig. 4 (A) SEM image and particle size of *R. hastatus* based AgNPs (B) EDS spectrum of *R. hastatus* based AgNPs.

anti-angiogenic, anti-tumor and anti-cholinesterase properties (Ahmed et al., 2016) of *R. hastatus* might be due to the high phenolic content. Similarly, total flavonoids content was also found high in crude leaf extract which asserted the leaves of study plant a good food material and drug for the treatment of pathogenic diseases (Ahmad et al., 2015, Baba and Malik 2015). High phenolic and flavonoid content of crude extracts of *R. hastatus* leaves is directly associated with high DPPH scavenging activity *i.e.,* increased antioxidant potential (Sulaiman and Balachandran 2012). DPPH scavenging activity was observed as 88 % in methanolic extract that is considered very good for health (Sahreen et al., 2011). Thus *R. hastatus* can be used to treat numerous diseases including several neurodegenerative diseases (Sahreen et al., 2014).

Present study has revealed that crude extract of *R. hastatus* leaf strongly inhibited the growth of tested strains in broth dilution method as compared to well diffusion method. Broth dilution method got advantage over the diffusion techniques due to its reproducibility; sensitivity and direct interaction of pathogens with plant extract (Balouiri et al., 2016). Using broth dilution method, number of viable cells have been observed (Albabtain et al., 2017) that's why % inhibition was observed to be high in tested strains which showed inverse pattern with well diffusion method. This might be due to the fact that plant extract directly interacts with pathogenic bacteria in broth dilution method while in well diffusion method plant extract interact with bacteria via diffusion. Overall results of antibacterial activity using both antibacterial assays have revealed that gram negative bacteria were more sensitive to *R. hastatus* leaf extracts compared to gram positive bacteria. This is due to the resistance caused by thick peptidoglycan layer in cell wall of gram positive bacteria (Pazos-Ortiz et al., 2017). Current study has revealed that methanolic extract of *R. hastatus* leaf has immense ability to inhibit the growth of applied bacterial strains. (Hussain et al., 2010) and Hussain *etal.,* 2010 also predicted the similar trend of antibacterial activity of *R. hastatus* leaves against human pathogenic bacteria (Hazrat et al., 2013, Hussain et al., 2010). Literature has shown that medicinal plant extracts attribute to the inhibition of essential macromolecules synthesis which modify the physiological factors of the bacterial cell and cause death of bacteria (Saritha et al., 2015). Due to detergent like properties, plant extract can cause the disruption of membrane potential, followed by leakage of cellular matrix (Pieme et al., 2014, Chi-Chen et al., 2012).

Silver ion and silver compounds are toxic to microorganisms and they usually have large surface area (Sökmen et al., 2017). Plant extracts act as reducing agent for the synthesis of silver nanoparticles (green synthesis of nanoparticles), more valuable than other biological processes (Valli and Vaseeharan 2012). The mechanism involve in the synthesis of AgNPs is the interaction of silver ions with secondary metabolites to get reduce by them, lead to formation of silver nuclei (Chung et al., 2016). In current research, we have successfully synthesized AgNPs using aqueous leaf extract of *R. hastatus*. Synthesis of AgNPs was asserted by the development of dark brown color (Imtiaz et al., 2017) from milky solution owing to the surface plasmon resonance (SPR) with absorption maxima at 367 nm. A number of previous studies reported the absorption maxima for AgNPs ranged from 350 nm to 490 nm (Ahmed et al., 2016, Solgi 2014, Rajeshkumar and Bharath 2017, Sarkar and Paul 2017). In XRD peaks of sythesized AgNPs were recorded at five Bragg's reflections *i.e.* 29.70°, 32.83°, 39.14°, 53.84° and 62.04° which indicated the spherical structure of AgNPs (Ahmed et al., 2016, Solgi 2014, Rajeshkumar and Bharath 2017, Sarkar and Paul 2017). The average crystalline size of AgNPs 85 nm in our study is in association with reported data (Jyoti et al., 2016, Marimuthu et al., 2011, Tareq et al., 2017). Presented X-ray diffraction pattern clearly indicates that AgNPs, synthesized by *R. hastatus* leaf extract, are crystalline in nature.

FTIR spectrum showed stretching frequencies at five different regions. The band at 3215 cm^{-1} attribute to O—H stretching vibration to carboxylic acid (Sonker et al., 2017,

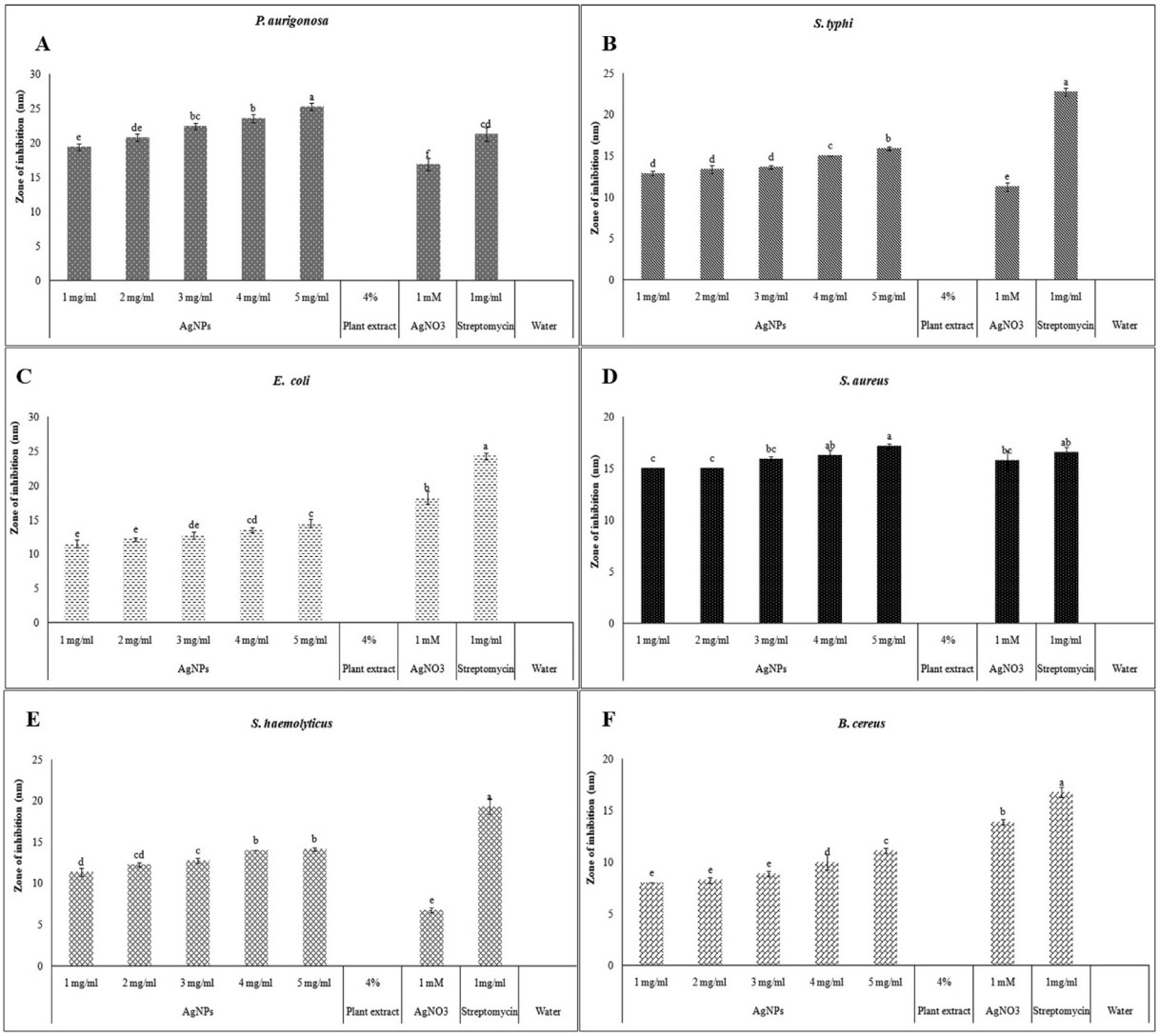

Fig. 5 Zone of inhibition induced by *R. hastatus* based AgNPs at 1–5 mg / ml compared with, aqueous leaf extract, $AgNO_3$, streptomycin and water against A) *P. aeruginosa;* B) *S. typhi;* C) *E. coli;* D) *S. aureus*; E) *S. haemoliticus* and F) *B. cereus*. Different letters on the bars revealed the significant difference ($P < 0.05$) between the zone of inhibition of bacteria at different concentrations of AgNPs and positive and negative controls.

Vijayaraghavan et al., 2012). The peak located at 2364 cm^{-1} assign to C═O or N─H stretching vibrations (Marimuthu et al., 2011). The peak at 1580 cm^{-1} can be corresponding to C═C stretching vibration (Marimuthu et al., 2011, Amooaghaie et al., 2015). The peak at 1290 cm^{-1} is known to be associated with C─O stretching vibration (da Silva Ferreira et al., 2017). The peak at 800 cm^{-1} corresponds to C─Cl stretching to alkyl halides (Geethalakshmi and Sarada 2010). Overall, FTIR analysis indicated that biomolecules (flavonoids and terpenoids) are the major components that are responsible for capping and stabilization of AgNPs (Gnanajobitha et al., 2013) synthesized by *R. hastatus* leaf extract.

Surface topography and morphology of *R. hastatus* based AgNPs was examined using Scanning Electron Microscope (SEM). All synthesized nanoparticles were spherical to semi spherical in shape. Fig. 4 showed the presence of some larger particles which may be generated due to the agglomeration of smaller particles during preparation of sample in drying process (Amooaghaie et al., 2015, Rajesh et al., 2017).The average size of the synthesized silver nanoparticles was 51 nm and ranged from 46 to 60 nm. The size of the *R. hastatus* based AgNPs met with the size of AgNPs synthesized by (Vijay Kumar et al., 2014) from *Madhuca longifolia, Cardiospermum helicacabum, Phoenix sylvestris L.* and *Thymus kotschyanus*. The size of the crystals differed from the average particle size, as the size of the crystals indicated the size of the repeating unit cells in a crystal lattice, whereas the particle size revealed the physical dimension of an individual particle (Kouhbanani et al., 2019). EDS analysis of synthesized AgNPs revealed the strong signals of metallic silver in the synthesized AgNPs (Patil et al., 2018, Mitra et al., 2012, Qidwai et al., 2018, Hamelian et al., 2018) along with small percentage of Nitrogen and Oxygen showed the material synthesized from biological route (Oves et al., 2022, Naveed et al., 2022).

Antibacterial activity of synthesized silver nanoparticles was carried out by well diffusion method at five different concentra-

tions *i.e* 1–5 mg/ml, which showed direct proportion between synthesized AgNPs concentration and related antibiotic activity. This research work elaborated the synergistic antibiotic activity of AgNPs that is higher than the individual antibacterial activity of $AgNO_3$ and plant extract which is in association with (da Silva Ferreira et al., 2017, Raja et al., 2017). The actual mode of action behind the antibacterial activity of AgNPs is still a topic of debate. Different studies proposed different mechanisms of antibacterial activity of AgNPs. A study revealed that antibiotic activity of AgNPs is due to the interaction of positively charged AgNPs and negatively charged bacterial cell (Malabadi et al., 2015, Pallela et al., 2018, Cao et al., 2001) which enhance the permeability of bacterial cell and ultimately cause death of bacteria (Cao et al., 2001, Wright et al., 1999, Eby et al., 2009). Literature also reported that all bactericidal activity of AgNPs attributed to the positively charged silver ion interaction with nucleic acid specifically with nucleoside to replace phosphate group, development of resulting silver containing compounds have observed bactericidal potential (Sondi and Salopek-Sondi 2004, Ahmed et al., 2016). A proteomic study proposed that AgNPs, after being oxidized by reacting with biomolecules (Ankanna et al., 2010), have greater affinity for membrane enzymes and disrupt the binding activity of enzyme to its substrate. These enzymes maintain the *trans*-membrane energy generation and transportation of ions (Wigginton et al., 2010). Synthesis of cell wall was also inhibited by the disruption of *trans*-membrane proteins function due to AgNPs interaction which leads the cell towards death by ATP leakage (Park et al., 2011).

5. Conclusion

The results of the present research have clinched that *R. hastatus* based AgNPs could be synthesized, characterized and used against pathogenic bacterial strains successfully as compared to crude leaf extracts of *R. hastatus*. On the bases of this research, the methanolic plant extracts contains high phenolic, flavonoid contents and antioxidant activity as compared to hexane extract and it could be used along with AgNPs for efficient therapeutic management of infectious pathogens.

6. Authors' contributions

SR conducted experiments, collected and analyze data, write original draft. RA, MA, SAK and AMA were involved in conceptualization, supervision, study design, data analysis and interpretation, and writing and reviewing the final draft. DAA and MSE revise manuscript, visualize data and provided financial assistance. All authors have read and approved the final manuscript.

Declaration of Competing Interest

The authors declare that they have no known competing financial interests or personal relationships that could have appeared to influence the work reported in this paper.

Acknowledgment

The authors would like to extend their sincere appreciation to the Researchers supporting Project number RSP2023R190, King Saud University, Riyadh, Saudi Arabia. In addition, research facilities provided by COMSATS University Islamabad, Abbottabad Campus are thankfully accredited.

References

Adebayo, A., Tan, N.-H., Akindahunsi, A., Zeng, G.-Z., Zhang, Y.-M., 2010. Anticancer and antiradical scavenging activity of Ageratum conyzoides L. (Asteraceae). Pharmacogn. Mag. 6, 62.

Ahmad, S., Ullah, F., Ayaz, M., Sadiq, A., Imran, M., 2015. Antioxidant and anticholinesterase investigations of Rumex hastatus D. Don: potential effectiveness in oxidative stress and neurological disorders. Biol. Res. 48, 20.

Ahmed, S., Ahmad, M., Swami, B.L., Ikram, S., 2016. A review on plants extract mediated synthesis of silver nanoparticles for antimicrobial applications: a green expertise. J. Adv. Res. 7, 17–28.

Ahmed, N., Mahmood, A., Ashraf, A., Bano, A., Tahir, S., Mahmood, A., 2015. Ethnopharmacological relevance of indigenous medicinal plants from district Bahawalnagar, Punjab, Pakistan. J. Ethnopharmacol. 175, 109–123.

Albabtain, R., Azeem, M., Wondimu, Z., Lindberg, T., Borg-Karlson, A.K., Gustafsson, A., 2017. Investigations of a possible chemical effect of salvadora persica chewing sticks. Evid. Based Complement. Alternat. Med. 2017, 10. https://doi.org/10.1155/2017/2576548.

Alharbi, N.S., Alsubhi, N.S., Felimban, A.I., 2022. Green synthesis of silver nanoparticles using medicinal plants: characterization and application. J. Radiat. Res. Appl. Sci. 15, 109–124.

Amooaghaie, R., Saeri, M.R., Azizi, M., 2015. Synthesis, characterization and biocompatibility of silver nanoparticles synthesized from Nigella sativa leaf extract in comparison with chemical silver nanoparticles. Ecotoxicol. Environ. Saf. 120, 400–408.

Ankanna, S.T., Prasad, T.N., Elumalai, E.K., Savithramma, N., 2010. Production of biogenic silver nanoparticles using Boswellia ovalifoliolata stem bark. Dig. J. Nanomater. Biostruct. 5, 369–372.

Ashebir, M., Ashenafi, M., 2007. Assessment of the antibacterial activity of some traditional medicinal plants on some food-borne pathogens. Ethiop. J. Health Dev. 32, 1999.

Baba, S.A., Malik, S.A., 2015. Determination of total phenolic and flavonoid content, antimicrobial and antioxidant activity of a root extract of Arisaema jacquemontii Blume. J. Taibah Univ. Sci. 9, 449–454.

Balouiri, M., Sadiki, M., Ibnsouda, S.K., 2016. Methods for in vitro evaluating antimicrobial activity: a review. J. Pharm. Anal. 6, 71–79.

Bennour, N., Mighri, H., Eljani, H., Zammouri, T., Akrout, A., 2020. Effect of solvent evaporation method on phenolic compounds and the antioxidant activity of Moringa oleifera cultivated in Southern Tunisia. S. Afr. J. Bot. 129, 181–190.

Calixto, J.B., 2005. Twenty-five years of research on medicinal plants in Latin America: a personal view. J. Ethnopharmacol. 100, 131–134.

Cao, Y., Jin, R., Mirkin, C.A., 2001. DNA-modified core− shell Ag/Au nanoparticles. J. Am. Chem. Soc. 123, 7961–7962.

Chakravarty, A., Ahmad, I., Singh, P., Ud Din Sheikh, M., Aalam, G., Sagadevan, S., Ikram, S., 2022. Green synthesis of silver nanoparticles using fruits extracts of Syzygium cumini and their bioactivity. Chem. Phys. Lett. 795,. https://doi.org/10.1016/j.cplett.2022.139493 139493.

Chauhan, S., Singh, M., Thakur, A., Dogra, M.S., 2017. Antibacterial activity of Nerium indicum against some Gram positive bacterial species. Int. J. Drug Res. Technol. 3, 3.

Chen, H.-H. and J.-H. Zhou, 2022. Systematic Investigation on $AlCl_3$ colorimetric determination of total flavonoids in daylily. In: International Conference on Biomedical and Intelligent Systems (IC-BIS 2022), SPIE.

Chi-Chen, Y., Yang, J.-I., Lee, J.-C., Tseng, C.-N., Chan, Y.-C., Hseu, Y.-C., Tang, J.-Y., Chuang, L.-Y., Huang, H.-W., Chang, F.-R.,

Chang, 2012. Anti-proliferative effect of methanolic extract of Gracilaria tenuistipitata on oral cancer cells involves apoptosis, DNA damage, and oxidative stress. BMC Complement. Altern. Med. 12, 142. https://doi.org/10.1186/1472-6882-12-142.

Chung, I.-M., Park, I., Seung-Hyun, K., Thiruvengadam, M., Rajakumar, G., 2016. Plant-mediated synthesis of silver nanoparticles: their characteristic properties and therapeutic applications. Nanoscale Res. Lett. 11, 40.

Croxen, M.A., Law, R.J., Scholz, R., Keeney, K.M., Wlodarska, M., Finlay, B.B., 2013. Recent advances in understanding enteric pathogenic Escherichia coli. Clin. Microbiol. Rev. 26, 822–880.

da Silva Ferreira, V., ConzFerreira, M.E., Lima, L.M.T.R., Frasés, S., de Souza, W., Sant'Anna, C., 2017. Green production of microalgae-based silver chloride nanoparticles with antimicrobial activity against pathogenic bacteria. Enzyme Microb. Technol. 97, 114–121. https://doi.org/10.1016/j.enzmictec.2016.10.018.

De Ghosh, M., Ramakrishna, S., Ramakrishna, T., 2014. Animicrobial activity and phytochemical analysis of medicinal plants. World J. Pharm. Pharm. Sci. 3, 1794–1799.

Dildora Ergashevna, K., Honbuvi Khakimovna, K., 2022. Current perspectives on the subject of public health and heath care. World Bulletin of Public Health. 6, 51–53.

Eby, D.M., Schaeublin, N.M., Farrington, K.E., Hussain, S.M., Johnson, G.R., 2009. Lysozyme catalyzes the formation of antimicrobial silver nanoparticles. ACS Nano 3, 984–994.

Geethalakshmi, R., Sarada, D., 2010. Synthesis of plant-mediated silver nanoparticles using Trianthema decandra extract and evaluation of their anti microbial activities. Int. J. Eng. Sci. Technol. 2, 970–975.

Gellatly, S.L., Hancock, R.E., 2013. Pseudomonas aeruginosa: new insights into pathogenesis and host defenses. Pathogens and Disease. 67, 159–173.

Gnanajobitha, G., Rajeshkumar, S., Kannan, C., Annadurai, G., 2013. Preparation and characterization of fruit-mediated silver nanoparticles using pomegranate extract and assessment of its antimicrobial activity. J. Environ. Nanotechnol. 2, 04–10.

Gökşen Tosun, N., Kaplan, Ö., Türkekul, İ., Gökçe, İ., Özgür, A., 2022. Green synthesis of silver nanoparticles using Schizophyllum commune and Geopora sumneriana extracts and evaluation of their anticancer and antimicrobial activities. Part. Sci. Technol. 40, 801–811. https://doi.org/10.1080/02726351.2021.2010846.

Gulia, K., James, A., Pandey, S., Dev, K., Kumar, D., Sourirajan, A., 2022. Bio-Inspired smart nanoparticles in enhanced cancer theranostics and targeted drug delivery. J. Functional Biomater. 13, 207.

Gunn, B.A., Davis, C.E., 1988. Staphylococcus haemolyticus urinary tract infection in a male patient. J. Clin. Microbiol. 26, 1055–1057.

Habeeb Rahuman, H.B., Dhandapani, R., Narayanan, S., Palanivel, V., Paramasivam, R., Subbarayalu, R., Thangavelu, S., Muthupandian, S., 2022. Medicinal plants mediated the green synthesis of silver nanoparticles and their biomedical applications. IET Nanobiotechnol. 16, 115–144.

Hameed, I., Dastagir, G., 2009. Nutritional analyses of Rumex hastatus D. Don, Rumex dentatus Linn and Rumex nepalensis Spreng. Afr. J. Biotechnol. 8, 131–133.

Hamelian, M., Zangeneh, M.M., Amisama, A., Varmira, K., Veisi, H., 2018. Green synthesis of silver nanoparticles using Thymus kotschyanus extract and evaluation of their antioxidant, antibacterial and cytotoxic effects. Appl. Organomet. Chem., e4458

Hazrat, A., Nisar, M., Zaman, S., 2013. Antibacterial activities of sixteen species of medicinal plants reported from Dir Kohistan Valley KPK, Pakistan. Pakistan J. Botany 45, 1369–1374.

Hussain, F., Ahmad, B., Hameed, I., Dastagir, G., Sanaullah, P., Azam, S., 2010. Antibacterial, antifungal and insecticidal activities of some selected medicinal plants of polygonaceae. Afr. J. Biotechnol. 9, 5032–5036.

Ibrahim, H.M., 2015. Green synthesis and characterization of silver nanoparticles using banana peel extract and their antimicrobial activity against representative microorganisms. J. Radiat. Res. Appl. Sci. 8, 265–275.

Ijaz, I., Bukhari, A., Gilani, E., Nazir, A., Zain, H., Saeed, R., Hussain, S., Hussain, T., Bukhari, A., Naseer, Y., Aftab, R., 2022. Green synthesis of silver nanoparticles using different plants parts and biological organisms, characterization and antibacterial activity. Environ. Nanotechnol. Monit. Manage. 18, 100704.

Imtiaz, M., Hamid, L., Ibrahim, M., Ahmad, Z., Kashif, M., Khan, I., Iqbal, M., 2017. Potent antibacterial activity of biogenic silver nanoparticles synthesized from Cassia fistula fruit. Microb. Pathog. 107, 354–360.

Jadhav, K., Dhamecha, D., Bhattacharya, D., Patil, M., 2016. Green and ecofriendly synthesis of silver nanoparticles: Characterization, biocompatibility studies and gel formulation for treatment of infections in burns. J. Photochem. Photobiol. B Biol. 155, 109–115.

Jain, N., Jain, P., Rajput, D., Patil, U.K., 2021. Green synthesized plant-based silver nanoparticles: therapeutic prospective for anticancer and antiviral activity. Micro Nano Syst. Lett. 9, 5. https://doi.org/10.1186/s40486-021-00131-6.

Jyoti, K., Baunthiyal, M., Singh, A., 2016. Characterization of silver nanoparticles synthesized using Urtica dioica Linn. leaves and their synergistic effects with antibiotics. J. Radiat. Res. Appl. Sci. 9, 217–227.

Kaplan, Ö., Gökşen Tosun, N., Özgür, A., Erden Tayhan, S., Bilgin, S., Türkekul, İ., Gökce, İ., 2021. Microwave-assisted green synthesis of silver nanoparticles using crude extracts of Boletus edulis and Coriolus versicolor: Characterization, anticancer, antimicrobial and wound healing activities. J. Drug Delivery Sci. Technol. 64,. https://doi.org/10.1016/j.jddst.2021.102641 102641.

Kaplan, Ö., Gökşen Tosun, N., İmamoğlu, R., Türkekul, İ., Gökçe, İ., Özgür, A., 2022. Biosynthesis and characterization of silver nanoparticles from Tricholoma ustale and Agaricus arvensis extracts and investigation of their antimicrobial, cytotoxic, and apoptotic potentials. J. Drug Delivery Sci. Technol. 69, 103178.

Kayani, S., Ahmad, M., Zafar, M., Sultana, S., Khan, M.P.Z., Ashraf, M.A., Hussain, J., Yaseen, G., 2014. Ethnobotanical uses of medicinal plants for respiratory disorders among the inhabitants of Gallies-Abbottabad, Northern Pakistan. J. Ethnopharmacol. 156, 47–60.

Khan, M.S., Ranjani, S., Hemalatha, S., 2022. Synthesis and characterization of Kappaphycus alvarezii derived silver nanoparticles and determination of antibacterial activity. Mater. Chem. Phys. 282, 125985.

Kotiranta, A., Lounatmaa, K., Haapasalo, M., 2000. Epidemiology and pathogenesis of Bacillus cereus infections. Microbes Infect. 2, 189–198.

Kouhbanani, M.A.J., Beheshtkhoo, N., Fotoohiardakani, G., Hosseini-Nave, H., Taghizadeh, S., Amani, A.M., 2019. Green synthesis and characterization of spherical structure silver nanoparticles using wheatgrass extract. J. Environ. Treatment Techniques. 7, 142–149.

Li, C.-C., Chang, S.-J., Su, F.-J., Lin, S.-W., Chou, Y.-C., 2013. Effects of capping agents on the dispersion of silver nanoparticles. Colloids Surf. A Physicochem. Eng. Asp 419, 209–215.

Lulekal, E., Asfaw, Z., Kelbessa, E., Van Damme, P., 2013. Ethnomedicinal study of plants used for human ailments in Ankober District, North Shewa Zone, Amhara region, Ethiopia. J. Ethnobiol. Ethnomed. 9, 63.

Malabadi, R.B., Mulgund, G.S., Meti, N.T., Nataraja, K., Kumar, S. V., 2015. Antibacterial activity of silver nanoparticles synthesized by using whole plant extracts of Clitoria ternatea. J. Res. Pharm. 2.

Marimuthu, S., Rahuman, A.A., Rajakumar, G., Santhoshkumar, T., Kirthi, A.V., Jayaseelan, C., Bagavan, A., Zahir, A.A., Elango, G., Kamaraj, C., 2011. Evaluation of green synthesized silver nanoparticles against parasites. Parasitol. Res. 108, 1541–1549. https://doi.org/10.1007/s00436-010-2212-4.

Martínez-Higuera, A., Rodríguez-Beas, C., Villalobos-Noriega, J.M. A., Arizmendi-Grijalva, A., Ochoa-Sánchez, C., Larios-Rodríguez,

E., Martínez-Soto, J.M., Rodríguez-León, E., Ibarra-Zazueta, C., Mora-Monroy, R., Borbón-Nuñez, H.A., García-Galaz, A., Candia-Plata, M.d.C., López-Soto, L.F., Iñiguez-Palomares, R., 2021. Hydrogel with silver nanoparticles synthesized by Mimosa tenuiflora for second-degree burns treatment. Sci. Rep. 11, 11312.

Martins, G.R., Monteiro, A.F., Amaral, F.R.L.do, da Silva, A.S.A., 2021. A validated Folin-Ciocalteu method for total phenolics quantification of condensed tannin-rich açaí (Euterpe oleracea Mart.) seeds extract. J. Food Sci. Technol., 1–10

Marzano, A., Mercogliano, M., Borghi, A., Facchetti, M., Caputo, R., 2003. Cutaneous infection caused by Salmonella typhi. J. Eur. Acad. Dermatol. Venereol. 17, 575–577.

Mitra, B., Vishnudas, D., Sant, S.B., Annamalai, A., 2012. Green-synthesis and characterization of silver nanoparticles by aqueous leaf extracts of Cardiospermum helicacabum leaves. Drug Invention Today. 4, 340–344.

Naveed, M., Batool, H., Rehman, S.U., Javed, A., Makhdoom, S.I., Aziz, T., Mohamed, A.A., Sameeh, M.Y., Alruways, M.W., Dablool, A.S., Almalki, A.A., Alamri, A.S., Alhomrani, M., 2022. Characterization and evaluation of the antioxidant, antidiabetic, anti-inflammatory, and cytotoxic activities of silver nanoparticles synthesized using Brachychiton populneus leaf extract. Processes 10, 1521.

Ogbuewu, I.P., Unamba-Oparah, I.C., Odoemenam, V.U., Etuk, I.F., Okoli, I.C., 2011. The potentiality of medicinal plants as the source of new contraceptive principles in males. N. Am. J. Med. Sci. 3, 255.

Oves, M., Ahmar Rauf, M., Aslam, M., Qari, H.A., Sonbol, H., Ahmad, I., Sarwar Zaman, G., Saeed, M., 2022. Green synthesis of silver nanoparticles by Conocarpus Lancifolius plant extract and their antimicrobial and anticancer activities. Saudi J. Biol. Sci. 29, 460–471. https://doi.org/10.1016/j.sjbs.2021.09.007.

Pallela, P., Ummey, S., Ruddaraju, L.K., Pammi, S.V.N., Yoon, S.G., 2018. Ultra Small, mono dispersed green synthesized silver nanoparticles using aqueous extract of Sida cordifolia plant and investigation of antibacterial activity. Microb. Pathog. 124, 63–69.

Park, J., Lim, D.-H., Lim, H.-J., Kwon, T., Choi, J.-S., Jeong, S., Choi, I.-H., Cheon, J., 2011. Size dependent macrophage responses and toxicological effects of Ag nanoparticles. Chem. Commun. 47, 4382–4384. https://doi.org/10.1039/c1cc10357a.

Patil, M., Singh, R., Koli, P., Tumadu Patil, K., Sonu Jagdale, B., Rajesh Tipare, A., Kim, G.-D., 2018. Antibacterial potential of silver nanoparticles synthesized using Madhuca longifolia flower extract as a green resource. Microb. Pathog. 121, 184–189. https://doi.org/10.1016/j.micpath.2018.05.040.

Pazos-Ortiz, E., Roque-Ruiz, J.H., Hinojos-Márquez, E.A., López-Esparza, J., Donohué-Cornejo, A., Cuevas-González, J.C., Espinosa-Cristóbal, L.F., Reyes-López, S.Y., 2017. Dose-Dependent antimicrobial activity of silver nanoparticles on polycaprolactone fibers against gram-positive and gram-negative bacteria. J. Nanomater.

Petrovska, B.B., 2012. Historical review of medicinal plants' usage. Pharmacogn. Rev. 6, 1.

Pieme, A., Guru Kumar, S., Sylviane, D., Bruno, M.M., Boyom, F., Yonkeu Ngogang, J., Saxena, A., 2014. Antiproliferative activity and induction of apoptosis by Annona muricata (Annonaceae) extract on human cancer cells. BMC Complement. Altern. Med. 14, 516. https://doi.org/10.1186/1472-6882-14-516.

Prasad, K.S., Pathak, D., Patel, A., Dalwadi, P., Prasad, R., Patel, P., Selvaraj, K., 2011. Biogenic synthesis of silver nanoparticles using Nicotiana tobaccum leaf extract and study of their antibacterial effect. Afr. J. Biotechnol. 10, 8122.

Prasad, R., Swamy, V.S., 2013. Antibacterial activity of silver nanoparticles synthesized by bark extract of Syzygium cumini. J. Nanoparticles.

Prasad, R., Swamy, V.S., Varma, A., 2012. Biogenic synthesis of silver nanoparticles from the leaf extract of Syzygium cumini (L.) and its antibacterial activity. Int. J. Pharm. Bio. Sci. 3, 745–752.

Qidwai, A., Kumar, R., Dikshit, A., 2018. Green synthesis of silver nanoparticles by seed of Phoenix sylvestris L. and their role in the management of cosmetics embarrassment. Green Chem. Lett. Rev. 11, 176–188.

Raja, S., Ramesh, V., Thivaharan, V., 2017. Green biosynthesis of silver nanoparticles using Calliandra haematocephala leaf extract, their antibacterial activity and hydrogen peroxide sensing capability. Arab. J. Chem. 10, 253–261. https://doi.org/10.1016/j.arabjc.2015.06.023.

Rajesh, V., Sophiya, J., Jacob, S.J.P., Arumugam, P., Jayaraman, P., 2017. Biosynthesis of silver nanoparticles using Diospyros ferrea (willd.) Bakh. leaves and evaluation of its antioxidant, anti-inflammatory, antimicrobial and anticancer activity. J. Bionanosci. 11, 24–33. https://doi.org/10.1166/jbns.2017.1408.

Rajeshkumar, S., Bharath, L., 2017. Mechanism of plant-mediated synthesis of silver nanoparticles–A review on biomolecules involved, characterisation and antibacterial activity. Chemico-Biological. Interactions.

Rezić, I., 2022. Nanoparticles for biomedical application and their synthesis. Polymers 14, 4961.

Roope, L.S.J., Smith, R.D., Pouwels, K.B., Buchanan, J., Abel, L., Eibich, P., Butler, C.C., Tan, P.S., Walker, A.S., Robotham, J.V., Wordsworth, S., 2019. The challenge of antimicrobial resistance: what economics can contribute. Science (New York, N.Y.) 364. https://doi.org/10.1126/science.aau4679.

Sahreen, S., Khan, M.R., Khan, R.A., 2011. Phenolic compounds and antioxidant activities of Rumex hastatus D. Don. Leaves. J. Medicinal Plants Res. 5, 2755–2765.

Sahreen, S., Khan, M.R., Khan, R.A., 2014. Comprehensive assessment of phenolics and antiradical potential of Rumex hastatus D Don. roots. BMC Complementary Alternative Med. 14, 47.

Saritha, K., Angireddy, R., Pujar, M., Setty, O.H., Yenugu, S., 2015. Mechanism of antibacterial action of the alcoholic extracts of Hemidesmus indicus (L.) R. Br. ex Schult, Leucas aspera (Wild.), Plumbago zeylanica L., and Tridax procumbens (L.) R. Br. ex Schult. Front. Microbiol. 6, 577. https://doi.org/10.3389/fmicb.2015.00577.

Sarkar, D., Paul, G., 2017. Synthesis of plant-mediated silver nanoparticles using commiphora wightii (guggul) extract and study their antibacterial activities against few selected organisms. World J. Pharm. Pharm. Sci. 6, 1418–1425.

Savithramma, N., Rao, M.L., Rukmini, K., Devi, P.S., 2011. Antimicrobial activity of silver nanoparticles synthesized by using medicinal plants. Int. J. ChemTech Res. 3, 1394–1402.

Sen, A., Batra, A., 2012. Evaluation of antimicrobial activity of different solvent extracts of medicinal plant: Melia azedarach L. Int. J. Curr. Pharm. Res. 4, 67–73.

Shakuntala, P., Bharti, D.N., Sachan, P.C., Gahlot, K., 2011. Evaluation of antidiarrhoeal activity of extract from roots of Rumex hastatus (family: Polygonaceae) on experimental animals. J. Appl. Pharm. Sci. 1, 182–185.

Sharma, V.K., Yngard, R.A., Lin, Y., 2009. Silver nanoparticles: green synthesis and their antimicrobial activities. Adv. Colloid Interface Sci. 145, 83–96.

Shimpi, S., Mahale, S., Chaudhari, D., Katkurwar, A., Bhandare, J., 2022. Copper nanoparticle-coated suture: a novel antimicrobial agent. J. Oral Res. Rev. 14, 104–108. https://doi.org/10.4103/jorr.jorr_47_21.

Singh, K., Panghal, M., Kadyan, S., Chaudhary, U., Yadav, J.P., 2014. Green silver nanoparticles of Phyllanthus amarus: as an antibacterial agent against multi drug resistant clinical isolates of Pseudomonas aeruginosa. J. Nanobiotechnol. 12, 40. https://doi.org/10.1186/s12951-014-0040-x.

Sökmen, M., Alomar, S.Y., Albay, C., Serdar, G., 2017. Microwave assisted production of silver nanoparticles using green tea extracts. J. Alloy. Compd. 725, 190–198.

Solgi, M., 2014. Evaluation of plant-mediated Silver nanoparticles synthesis and its application in postharvest physiology of cut Flowers. Physiol. Mol. Biol. Plants 20, 279–285.

Sondi, I., Salopek-Sondi, B., 2004. Silver nanoparticles as antimicrobial agent: a case study on E. coli as a model for Gram-negative bacteria. J. Colloid Interface Sci. 275, 177–182.

Sonker, A.S., Pathak, J., Kannaujiya, V.K., Sinha, R.P., 2017. Characterization and in vitro antitumor, antibacterial and antifungal activities of green synthesized silver nanoparticles using cell extract of Nostoc sp. strain HKAR-2. Can. J. Microbiol. 1, 26–37. https://doi.org/10.24870/cjb.2017-000103.

Sulaiman, C.T., Balachandran, I., 2012. Total phenolics and total flavonoids in selected Indian medicinal plants. Indian J. Pharm. Sci. 74, 258–260.

Tareq, F.K., Fayzunnesa, M., Kabir, M.S., 2017. Antimicrobial activity of plant-median synthesized silver nanoparticles against food and agricultural pathogens. Microb. Pathog. 109, 228–232. https://doi.org/10.1016/j.micpath.2017.06.002.

Valli, J.S., Vaseeharan, B., 2012. Biosynthesis of silver nanoparticles by Cissus quadrangularis extracts. Mater. Lett. 82, 171–173.

Vijay Kumar, P.P.N., Pammi, S.V.N., Kollu, P., Satyanarayana, K.V. V., Shameem, U., 2014. Green synthesis and characterization of silver nanoparticles using Boerhaavia diffusa plant extract and their anti bacterial activity. Ind. Crop. Prod. 52, 562–566. https://doi.org/10.1016/j.indcrop.2013.10.050.

Vijayaraghavan, K., Nalini, S.P.K., Prakash, N.U., Madhankumar, D., 2012. One step green synthesis of silver nano/microparticles using extracts of Trachyspermum ammi and Papaver somniferum. Colloids Surf. B Biointerfaces 94, 114–117. https://doi.org/10.1016/j.colsurfb.2012.01.026.

Wiegand, I., Hilpert, K., Hancock, R., 2007. Agar and broth dilution methods to determine the minimal inhibitory concentration (MIC) of antimicrobial substances. Nat. Protoc. 3, 163–175.

Wigginton, N.S., Titta, A.D., Piccapietra, F., Dobias, J., Nesatyy, V.J., Suter, M.J., Bernier-Latmani, R., 2010. Binding of silver nanoparticles to bacterial proteins depends on surface modifications and inhibits enzymatic activity. Environ. Sci. Tech. 44, 2163–2168.

Wright, J., Lam, K., Hansen, D., Burrell, R., 1999. Efficacy of topical silver against fungal burn wound pathogens. Am. J. Infect. Control 27, 344–350.

Yadav, R., Khare, R., Singhal, A., 2017. Qualitative Phytochemical Screening of Some Selected Medicinal Plants of Shivpuri District (MP). Int. J. Life Sci. Sci. Res. 3, 844–847.

Zhang, Y., Zhan, D.-S., Xu, X.-Y., Zhang, Z., Hafez, M.E., He, Y., Li, Y., Li, D.-W., 2023. Label-free detection of DNA methylation by surface-enhanced Raman spectroscopy using zirconium-modified silver nanoparticles. Talanta 253, 123941.